



**HAL**  
open science

## MRI-based kidney radiomic analysis during chronic lithium treatment

Paul Beunon, Maxime Barat, Anthony Dohan, Lynda Cheddani, Lisa Males, Pedro Fernandez, Bruno Etain, Frank Bellivier, Emeline Marlinge, François Vrtovsnik, et al.

► **To cite this version:**

Paul Beunon, Maxime Barat, Anthony Dohan, Lynda Cheddani, Lisa Males, et al.. MRI-based kidney radiomic analysis during chronic lithium treatment. *European Journal of Clinical Investigation*, 2022, 52 (5), pp.e13756. 10.1111/eci.13756 . inserm-03847183

**HAL Id: inserm-03847183**


**<https://inserm.hal.science/inserm-03847183v1>**

Submitted on 10 Nov 2022

**HAL** is a multi-disciplinary open access archive for the deposit and dissemination of scientific research documents, whether they are published or not. The documents may come from teaching and research institutions in France or abroad, or from public or private research centers.

L'archive ouverte pluridisciplinaire **HAL**, est destinée au dépôt et à la diffusion de documents scientifiques de niveau recherche, publiés ou non, émanant des établissements d'enseignement et de recherche français ou étrangers, des laboratoires publics ou privés.

# MRI-based kidney radiomic analysis during chronic lithium treatment

Paul Beunon<sup>1,2</sup> | Maxime Barat<sup>2,3</sup> | Anthony Dohan<sup>2,3</sup> | Lynda Cheddani<sup>4,5</sup> |  
 Lisa Males<sup>3,6</sup> | Pedro Fernandez<sup>6</sup> | Bruno Etain<sup>3,7</sup> | Frank Bellivier<sup>3,7</sup> |  
 Emeline Marlinge<sup>7</sup> | François Vrtovsnik<sup>3,7,8</sup> | Emmanuelle Vidal-Petiot<sup>3,7,9</sup> |  
 Antoine Khalil<sup>3,6</sup> | Jean-Philippe Haymann<sup>1,10</sup> | Martin Flamant<sup>3,7,9</sup> |  
 Nahid Tabibzadeh<sup>9,11,12</sup> 

<sup>1</sup>Sorbonne Université, Paris, France

<sup>2</sup>Radiologie A, APHP.Centre Hôpital Cochin, Paris, France

<sup>3</sup>Université de Paris, Paris, France

<sup>4</sup>Université Paris Saclay, INSERM U1018, Equipe 5, CESP (Centre de Recherche en Épidémiologie et Santé des Populations), Paris, France

<sup>5</sup>Néphrologie, APHP Hôpital Ambroise Paré, Paris, France

<sup>6</sup>Radiologie, APHP.Nord Hôpital Bichat, Paris, France

<sup>7</sup>Département de Psychiatrie et de Médecine Addictologique, APHP.Nord, GH Lariboisière-Fernand-Widal, DMU Neurosciences, Paris, France

<sup>8</sup>Néphrologie, APHP.Nord Hôpital Bichat, Paris, France

<sup>9</sup>Explorations Fonctionnelles, Physiologie, APHP.Nord Hôpital Bichat, Paris, France

<sup>10</sup>Explorations Fonctionnelles et laboratoire de la lithiase, APHP. Sorbonne Hôpital Tenon, Paris, France

<sup>11</sup>Centre de Recherche des Cordeliers, INSERM, Sorbonne Université, Université de Paris, Laboratoire de Physiologie Rénale et Tubulopathies, Paris, France

<sup>12</sup>CNRS ERL 8228–Unité Métabolisme et Physiologie Rénale, Paris, France

## Correspondence

Nahid Tabibzadeh, Physiologie rénale, explorations fonctionnelles, APHP.Nord Hôpital Bichat, Centre de Recherche des Cordeliers, Université de Paris, Paris U1138, France.

Email: [nahid.tabibzadeh@inserm.fr](mailto:nahid.tabibzadeh@inserm.fr)

## Abstract

**Background:** Lithium therapy during bipolar disorder is associated with an increased risk of chronic kidney disease (CKD) that is slowly progressive and undetectable at early stages. We aimed at identifying kidney image texture features as possible imaging biomarkers of decreased measured glomerular filtration rate (mGFR) using radiomics of T2-weighted magnetic resonance imaging (MRI).

**Methods:** One hundred and eight patients treated with lithium were evaluated including mGFR and kidney MRI, with T2-weighted sequence single-shot fast spin-echo. Computed radiomic analysis was performed after kidney segmentation. Significant features were selected to build a radiomic signature using multivariable Cox analysis to detect an mGFR <60 ml/min/1.73 m<sup>2</sup>. The texture index was validated using a training and a validation cohort.

**Results:** Texture analysis index was able to detect an mGFR decrease, with an AUC of 0.85 in the training cohort and 0.71 in the validation cohort. Patients

This is an open access article under the terms of the [Creative Commons Attribution-NonCommercial-NoDerivs](https://creativecommons.org/licenses/by-nc-nd/4.0/) License, which permits use and distribution in any medium, provided the original work is properly cited, the use is non-commercial and no modifications or adaptations are made.

© 2022 The Authors. *European Journal of Clinical Investigation* published by John Wiley & Sons Ltd on behalf of Stichting European Society for Clinical Investigation Journal Foundation

with a texture index below the median were older (59 [42–66] vs. 46 [34–54] years,  $p = .001$ ), with longer treatment duration (10 [3–22] vs. 6 [2–10] years,  $p = .02$ ) and a lower mGFR (66 [46–84] vs. 83 [71–94] ml/min/1.73m<sup>2</sup>,  $p < .001$ ). Texture analysis index was independently and negatively associated with age ( $\beta = -.004 \pm 0.001$ ,  $p < .001$ ), serum vasopressin ( $-0.005 \pm 0.002$ ,  $p = .02$ ) and lithium treatment duration ( $-0.01 \pm 0.003$ ,  $p = .001$ ), with a significant interaction between lithium treatment duration and mGFR ( $p = .02$ ).

**Conclusions:** A renal texture index was developed among patients treated with lithium associated with a decreased mGFR. This index might be relevant in the diagnosis of lithium-induced renal toxicity.

#### KEYWORDS

radiomics, magnetic resonance imaging, chronic kidney disease, lithium, bipolar disorder

## 1 | INTRODUCTION

Lithium carbonate is the cornerstone long-term treatment of bipolar disorder. The efficacy of lithium is proven in the prevention and treatment of acute maniac and depressive episodes and in the prevention of suicidal risk.<sup>1–3</sup> However this efficacy is counterbalanced by potentially serious adverse events. Even at therapeutic ranges long-term lithium treatment might lead to polyuria and polydipsia related to impaired urine concentrating ability and eventually to an increased risk of chronic kidney disease (CKD).<sup>4–6</sup>

Specific causal attribution of CKD to lithium treatment in this population is still controversial. Although some authors have related CKD to comorbidities such as ageing hypertension and metabolic syndrome in these patients<sup>7</sup> late-stage lithium-associated CKD is characterized by a typical pattern associating tubular atrophy interstitial fibrosis and diffuse cortical and/or medullary microcysts than can be evidenced on renal magnetic resonance imaging (MRI).<sup>8–11</sup> Moreover experimental models have shown structural changes early after lithium initiation characterized by cellular proliferation within renal collecting ducts.<sup>12,13</sup> To date these early changes cannot be detected through noninvasive tests. Yet the detection of lithium-induced early nephrotoxicity is of major importance when facing the issue of lithium discontinuation and would be helpful in weighing the risk/benefit ratio.

Radiomics is a growing field of research consisting of the mathematical integration of high-throughput data produced by medical imaging.<sup>14</sup> The image texture is analysed at the pixel scale allowing the computation of multiple data. Radiomic analyses have been shown to accurately detect the degree of cancer cell proliferation and heterogeneity within the tissue hence determining the prognosis of solid tumours.<sup>14</sup> It might thus represent a noninvasive surrogate biomarker of histological findings potentially allowing personalized management of patients. When

considering CKD kidney interstitial fibrosis has a highly predictive value irrespective of the underlying nephropathy.<sup>15,16</sup> Developing noninvasive methods in the management of patients with kidney disease is thus also of major importance.

In this view we hypothesized that noninvasive texture-based imaging biomarkers could provide quantifiable specific modification in patients treated with lithium carbonate and that it could detect an early decrease in measured glomerular filtration rate (GFR) in this population.

We thus aimed at developing a kidney MRI radiomic technique in patients treated with lithium and evaluating the correlates of kidney texture in this population.

## 2 | METHODS

### 2.1 | Design

In this retrospective, observational, single-centre study, one hundred and fourteen patients on chronic lithium treatment (at least 6 months) with available kidney MRI with T2-weighted coronal sequences were retrospectively included. Five patients were excluded from the analysis due to artefacts ( $n = 2$ ), inappropriate sequences ( $n = 1$ ), incomplete test ( $n = 1$ ) and solitary kidney ( $n = 1$ ) (study flowchart, [Figure 1](#)).

### 2.2 | Population

From March 2015 to December 2020, 109 adult patients were referred by psychiatrists to the Department of Renal Physiology for systematic check-up with nephrologists. Eligible patients were  $\geq 18$  years of age at inclusion, with various durations of lithium treatment and various doses, from 125 to 2400 mg per day, and no dialysis or kidney

FIGURE 1 Study flowchart

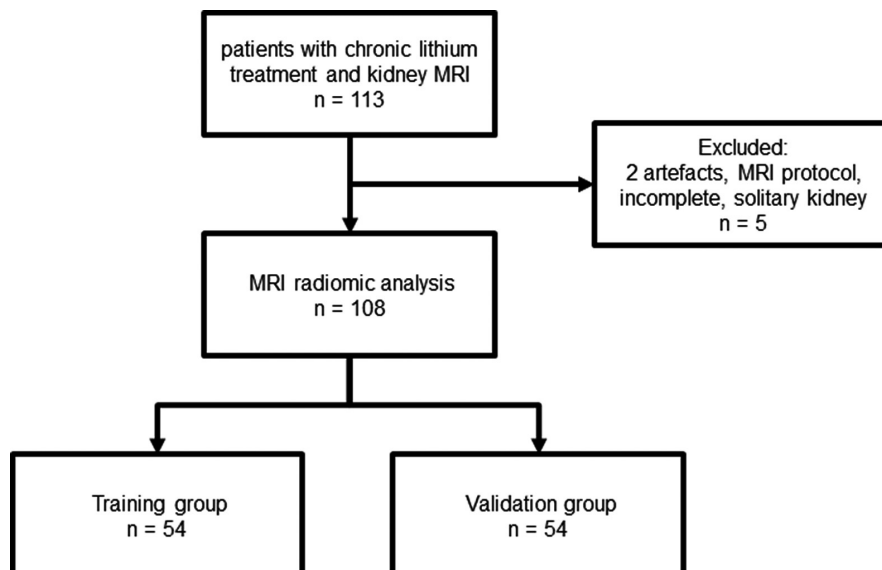
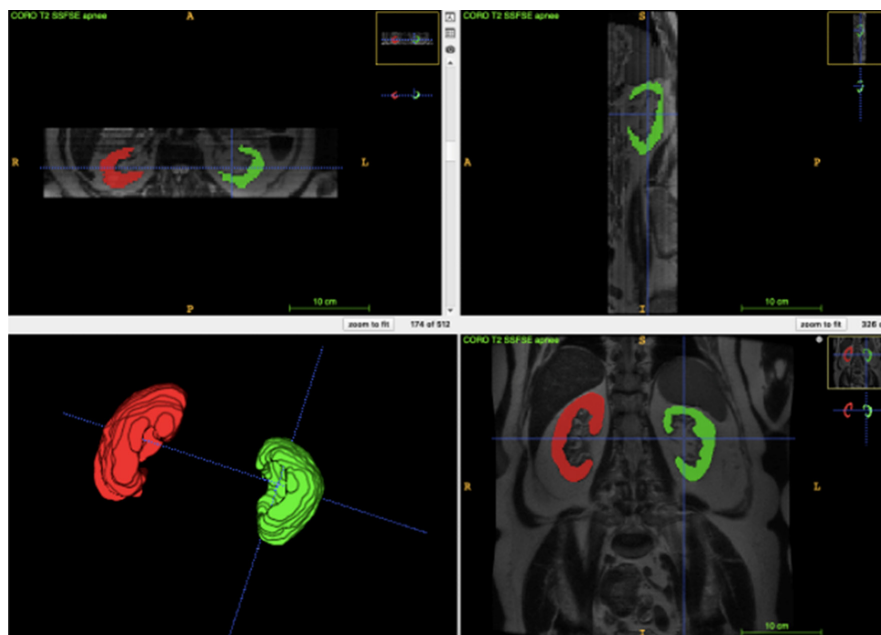


FIGURE 2 MRI manual renal segmentation on ITK SNAP 3.8.0



transplantation history. Among them, 23 patients had hypertension and 3 had diabetes mellitus. None of the patients had other causes of nephropathy, including glomerular diseases.

All patients provided written informed consent before inclusion in the study cohort. The study was approved by the local ethics committee (Institutional Review Board CER-2021-74), and Helsinki's Declaration ethical statements were respected.

### 2.3 | Data collection and measurements

During a half-day in-person visit, clinical and biological parameters were collected. GFR was measured (mGFR) by

urinary clearance of  $^{99}\text{Tc-DTPA}$  or  $^{51}\text{Cr-EDTA}$  (Curium, Saclay, France, and GE Healthcare, Velizy, France, respectively) as previously described.<sup>17</sup> Plasma lithium concentration was the last available measurement during the last 6 months. Serum vasopressin was measured by competition binding radioimmunological assay in the Renal Physiology Laboratory of Hôpital Tenon ( $1 < \text{normal value} < 5 \text{ pg/ml}$ ), France, with a standardized and validated protocol as described by Ho et al.<sup>18</sup> Desmopressin (dDAVP) was injected 2 h after the admission of the patient who remained fasting. Urine osmolality was measured using delta cryoscopy (Osmometer, Radiometer, Denmark). Maximal urine concentrating ability was defined as the highest value of urine osmolality among the measures performed on urine collected every 30 minutes

during 4 h (8 measures). Normal maximal urine concentrating ability is defined by a maximal urine osmolality above 600 mOsm/kgH<sub>2</sub>O.<sup>19</sup>

## 2.4 | Kidney MRI

We performed a standardized protocol using T2-weighted sequence single-shot fast spin-echo (SSFSE) without gadolinium enhancement. T2 SSFSE is an ultrafast MRI technique less susceptible to kinetic or respiratory artefacts and highly T2-weighted sequence allowing an optimal contrast between microcysts and renal parenchyma. MRI characteristics are reported in supplementary Table S1.

Kidney length was measured pole to pole. Cortex thickness was measured in the sagittal plane over the medullary pyramid facing the superior calyx, perpendicular to the cortical surface. Renal microcysts were defined as small (1–2 mm) round cystic lesions and quantified in both kidneys using a semi-quantitative scoring as previously described.<sup>8</sup> MRI voxel values were not normalized using the cerebrospinal liquid as all patients were examined on the same machine GE 3T and as voxel value-based features were excluded from the analysis.

Manual segmentation of renal parenchyma excluding sinus was performed using ITK SNAP 3.8.0. The software package has an interactive viewer that allows visualization in coronal, sagittal and axial planes (Figure 2). Finally, we extracted radiomic features using the pyradiomic module on 3D Slicer software 4.13.0. allowing the extraction of 107 first- and second-order features.<sup>20,21</sup>

## 2.5 | Statistical analyses

Using the Microsoft Office Excel randomization program = RAND(), the cohort was randomly split into a training cohort ( $n = 54$ ) and a validation cohort ( $n = 55$ ). All radiomic features were analysed and selected using penalized regression Lasso method.<sup>22</sup> A receiver operating characteristic (ROC) curve was plotted to measure the area under the curve (AUC), and the Youden index allowed identifying the most accurate cut-off value for the detection of an mGFR below 60 ml/min/1.73m<sup>2</sup>. Two first-order features relevant for the prediction of an mGFR below 60 ml/min/1.73m<sup>2</sup> were identified, namely, skewness and kurtosis, and the second-order features of the grey level co-occurrence matrix (GLCM) that were identified were correlation and cluster shade. Based on these features, we built a quantitative score using fitting generalized linear model, used as a texture analysis index.

Categorical variables were shown as frequencies and percentages, and quantitative variables were described

as median (quartile 1–quartile 3). Patients' characteristics were shown according to the texture analysis index above or below the median and compared using the chi-square test for categorical variables and the Mann-Whitney test for quantitative variables.

Determinants of texture analysis index were assessed using a multivariable linear regression stepwise model. Models were compared by maximum likelihood ratio test (nested models). Validity conditions of multiple linear regression models were checked. First, the model's suitability was tested using the rainbow test. We then studied the residuals. Their independence was checked using the Durbin-Watson test associated with a graphical method. A quantile-quantile plot was made to check their normal distribution. The distribution's homogeneity has been graphically checked by representing the square root of standardized residuals vs. fitted values. The following covariates were included *a priori* in the model: age, gender, hypertension, lithium treatment duration in years, mGFR, serum vasopressin and the interaction term between lithium treatment duration and mGFR.

A two-sided  $p$  value  $<.05$  was considered statistically significant. Statistical analyses and graphs were performed using GraphPad Prism 9.0 and R 3.4 software.

## 3 | RESULTS

### 3.1 | Texture analysis index validation and accuracy to detect mGFR $<60$ ml/min/1.73m<sup>2</sup>

We built a texture analysis index based on the first- and second-order features described above. This quantitative index was tested using an AUC to detect an mGFR  $<60$  ml/min/1.73 m<sup>2</sup> (Figure 3). The AUC was 0.85 in the training cohort and 0.71 in the validation cohort, with a Youden index at 0.66 in the training cohort and 0.67 in the validation cohort, showing a satisfying validation of the technique. Characteristics of the training and the validation cohorts were comparable (Table S2).

### 3.2 | Characteristics of the population

Characteristics of the studied population are reported in Table 1. Median age was 51 [38–63] years in the entire cohort, median lithium treatment duration was 7 [2.6–16] years and median mGFR was 77.7 [56.2–90.3] ml/min/1.73 m<sup>2</sup>. Compared to patients with a texture analysis index above the median, patients with a texture analysis index below the median were older (46 [34–54] vs. 59 [42–66] years,  $p = .001$ ), with a higher body mass index

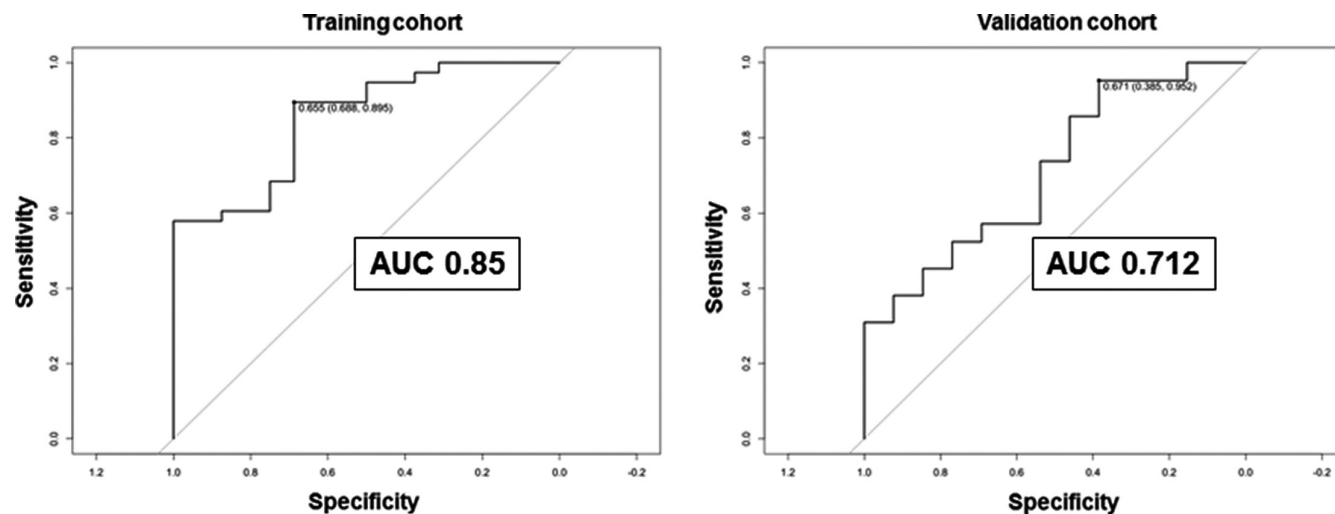


FIGURE 3 Receiver operating characteristic curve to detect mGFR <60 ml/min/1.73 m<sup>2</sup> in the training and the validation cohort

(BMI) (25.5 [22.6–27.4] vs. 27 [24.3–29.6] kg/m<sup>2</sup>,  $p = .01$ ), and had a longer lithium treatment duration (6 [2–10.3] vs. 10 [3.4–22.3] years,  $p = .02$ ), a lower daily lithium dose (800 [720–1200] vs. 750 [500–1000] mg/d,  $p = .04$ ), a lower maximal urine concentrating ability (701 [573–856] vs. 584 [328–793] mOsm/kgH<sub>2</sub>O,  $p = .01$ ) and more renal microcysts.

### 3.3 | Texture analysis index according to patients' characteristics

Texture analysis index was correlated with mGFR and age. The association remained significant between texture analysis index and age in the absence of microcysts ( $r^2 = .13$ ,  $p = .008$ ) but not for mGFR (Figure 4A–C). Regarding the relationship between texture analysis index and lithium treatment duration, the lowest tertile of texture analysis index was observed in the patients with the longest treatment duration (Figure 4D). Interestingly, the proportion of texture index within the medium tertile was the highest in patients treated with lithium for less than 5 years compared to longer treatment durations, whereas index within the highest tertile was found in patients treated with lithium for 5 to 15 years.

### 3.4 | Determinants of texture analysis index

Texture index was negatively associated with age ( $\beta -0.004 \pm 0.001$ ,  $p < .001$ ), lithium treatment duration ( $-0.01 \pm 0.003$ ,  $p = .001$ ) and serum vasopressin ( $-0.005 \pm 0.002$ ,  $p = .02$ ) independently of gender,

albuminuria and hypertension (Table 2). The association with mGFR vanished when lithium treatment duration was added to the model but with a significant interaction between treatment duration and mGFR ( $p = .01$ ).

## 4 | DISCUSSION

This study presents the first report of kidney MRI radiomics in patients treated with lithium carbonate. We built a texture analysis index that was associated with a decrease in mGFR. This texture index depended on lithium treatment duration and was independently associated with age, vasopressin level and mGFR.

Lithium nephrotoxicity remains a major clinical issue because of its slow, asymptomatic and unpredictable evolution, which can lead to end-stage kidney disease.<sup>23</sup> The benefit of lithium discontinuation, in particular, the reversibility of renal function alteration, and the probable individual susceptibility are currently debated.<sup>9,23,24</sup> Improved markers are, therefore, needed in these patients.

In our study, texture features were extracted from MR images and evaluated for their individual performance in detecting a mGFR below 60 ml/min/1.73m<sup>2</sup>. The first step was to validate the most relevant variables.

In a second step, we established a quantitative index allowing us to put it into the perspective of the patients' characteristics. We observed an association between this index and the duration of lithium exposure. The number of microcysts was also correlated with the texture analysis.

Multivariable analysis of the determinants of this index showed a negative association between texture index and age, independently of lithium treatment duration. One could hypothesize that ageing might modulate kidney texture, raising the potential interest of this marker

TABLE 1 Population characteristics in higher and lower structure index groups

	Overall population <i>n</i> = 08	≥Median structure index <i>n</i> = 54	<Median structure index <i>n</i> = 54	<i>p</i> -value
Age, years	51 [38–63]	46 [34–54]	59 [42–66]	<b>.001</b>
Male	43 (40)	20 (37)	23 (43)	.6
BMI, kg/m <sup>2</sup>	26 [23–29]	26 [23–27]	27 [24–30]	<b>.01</b>
Hypertension	29 (27)	13 (24)	16 (30)	.5
Diabetes	3 (3)	1 (2)	2 (4)	–
Hypothyroidism	33 (31)	15 (28)	18 (33)	.5
Lithium treatment duration, years	7 [2.6–16]	6 [2–10.3]	10 [3.4–22.3]	<b>.02</b>
Sustained-release formulation	68 (63)	34 (63)	34 (63)	1
Lithium dose, mg/day	800 [600–1000]	800 [720–1200]	750 [500–1000]	<b>.04</b>
Serum lithium level, mmol/l	0.7 [0.6–0.9]	0.7 [0.5–0.8]	0.7 [0.6–0.9]	.3
mGFR, ml/min/1.73m <sup>2</sup>	78 [56–90]	83 [71–94]	66 [46–84]	<b>&lt;.001</b>
ACR, mg/mmol	1.4 [0.9–2.6]	1.4 [0.9–2.3]	1.5 [0.9–2.6]	.7
Urine output, l/day	2.3 [1.7–3.2]	2.4 [1.9–3.2]	2.3 [1.6–3.5]	.5
Maximal urinary osmolality, mOsm/kgH <sub>2</sub> O	665 [480–839]	701 [573–856]	584 [328–793]	<b>.01</b>
Serum vasopressin, pg/ml	6.6 [4.4–12.3]	5.7 [4.0–10.0]	7.9 [4.6–13.4]	.08
Kidney MRI				
Number of cysts	0 [0–0]	0 [0–0]	0 [0–2]	–
Number of microcysts				
0	53 (49)	36 (67)	17 (31)	<b>.002</b>
1–5	25 (23)	9 (17)	16 (30)	
6–10	6 (6)	2 (4)	4 (7)	
11–20	6 (6)	3 (6)	3 (6)	
21–50	6 (6)	5 (9)	4 (7)	
51–100	3 (3)	1 (2)	2 (4)	
>100	9 (8)	1 (2)	8 (15)	
Structure analysis index	0.79 [0.66–0.86]	0.86 [0.82–0.90]	0.66 [0.48–0.74]	<b>&lt;.001</b>

Note: Categorical and continuous data are expressed in *n* (%) and in median [quartile 1– quartile 3], respectively. Patients' characteristics were compared across texture analysis index (above or below the median) using the chi-square test for categorical variables and Mann-Whitney for quantitative variables. Bold *p*-values are significant.

Abbreviations: ACR, urinary albumin-to-creatinine ratio; mGFR, measured glomerular filtration rate; MRI, magnetic resonance imaging.

when studying structural changes associated with renal senescence.

Texture analysis index was also negatively associated with serum vasopressin in our population. Previous research reported the potential adverse effects of vasopressin on CKD progression in various experimental models<sup>25</sup> and in polycystic kidney disease.<sup>26</sup> Elevated vasopressin levels in patients treated with lithium salts might reflect renal resistance to the action of vasopressin, eventually leading to decreased urine concentrating ability and nephrogenic diabetes insipidus.<sup>4</sup> In line with the pathophysiology of polycystic kidney disease in which vasopressin-dependent V2R signalling induces cellular proliferation and cyst

development,<sup>27</sup> these findings raise interesting hypotheses regarding the pathophysiology of lithium-associated microcystic tubulointerstitial nephropathy. Interestingly, previous report from Kline et al. showed that image texture changes during PKD-predicted CKD progression.<sup>28</sup>

Finally, the texture index was negatively associated with lithium treatment duration. Interestingly, the association with mGFR in multivariable analysis disappeared when lithium treatment duration was added to the model. Moreover, a significant interaction was found between lithium treatment duration and mGFR, suggesting that mGFR influences the relationship between kidney texture and lithium exposure. This result should be put in light

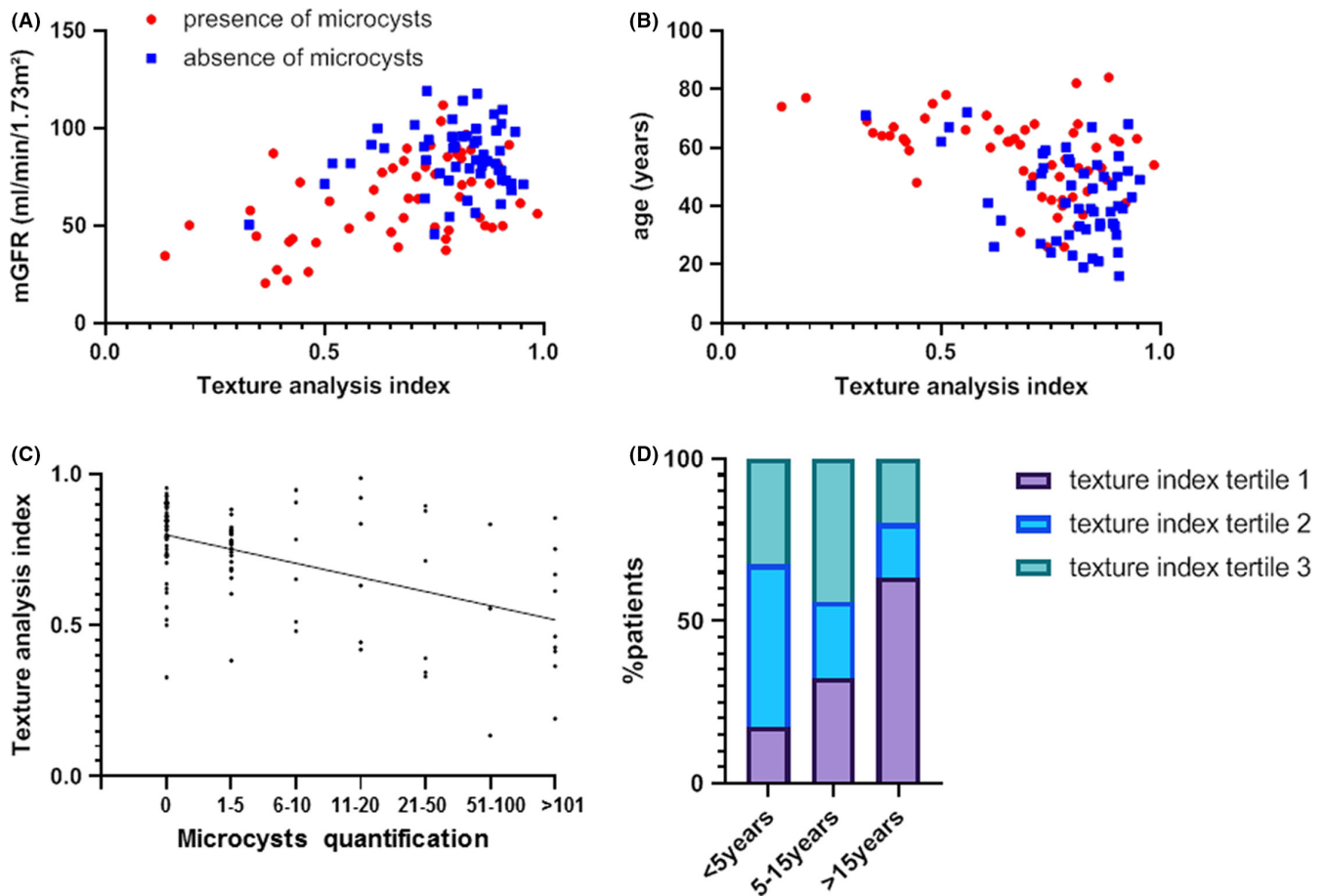


**FIGURE 4** Correlations of texture analysis indexes with patients' characteristics. Texture analysis index according to mGFR (A), to age (B) in patients with no microcysts (blue squares) and in patients with microcysts (red dots). Microcyst quantification according to texture analysis index (C). Texture analysis index tertiles according to lithium treatment duration (D)

**TABLE 2** Multivariable analysis of the determinants of texture analysis index

Dependent variable: texture index	$\beta \pm SE$	<i>p</i> value
Age	$-0.004 \pm 0.001$	<b>&lt;.001</b>
Lithium treatment duration	$-0.01 \pm 0.003$	<b>.001</b>
mGFR	$-0.0008 \pm 0.003$	.5
Serum vasopressin	$-0.005 \pm 0.002$	<b>.02</b>
mGFR*treatment duration interaction	-	<b>.01</b>

*Note:* Determinants were assessed using a multivariable linear regression stepwise model. The following variables were included in the model: age, gender, mGFR, lithium treatment duration, urine albumin/creatinine ratio, hypertension, interaction term between lithium treatment duration and mGFR. Bold *p*-values are significant.

with our previous report showing an independent and strong relationship between mGFR and lithium treatment duration.<sup>8</sup> However, the causative role of each variable is not yet demonstrated, and whether the texture index is specific to lithium nephrotoxicity or generalizable to

other causes of CKD remains to be elucidated. Besides the work from Kline et al. on PKD,<sup>28</sup> recent literature has investigated kidney texture analysis in kidney diseases such as glomerulonephritis<sup>29</sup> or radiation-induced kidney damage<sup>30</sup> and during CKD.<sup>31,32</sup> It has been shown that interstitial fibrosis is associated with worst renal outcome independently of GFR, in native kidneys and in kidney allografts.<sup>33–35</sup> In the perspective of identifying noninvasive biomarkers that correlate with renal fibrosis,<sup>36</sup> Berchtold et al.<sup>37</sup> and Friedli et al.<sup>38</sup> have developed an MR imaging tool to detect renal fibrosis using an apparent diffusion coefficient, demonstrating the utility of noninvasive diagnostic tools in CKD. To the best of our knowledge, there is no report of the association of histologically proven kidney interstitial fibrosis and radiomic analysis. Further research is, thus, needed to investigate this association globally during CKD.

We can identify some limitations to our study. First, our study included a small sample of patients, which nevertheless remains the largest cohort of lithium-treated patients with a standardized MRI protocol. Our study also lacks external validation on a control



population due to the specific MRI protocol used in these patients and the measurement of GFR, which is not routinely performed in patients with CKD. Finally, the cross-sectional design of our study does not allow evaluating the prognostic impact of our new biomarker. Our methodological validation with a gold-standard method of GFR measurement might, thus, be useful to future investigations including longitudinal follow-up of patients treated with lithium and patients with CKD. The identification of the most appropriate first- and second-order texture features that are correlated with CKD in our cohort may, thus, be used in other studies involving patients with CKD and during kidney transplantation. As kidney biopsy is still necessary to properly evaluate the renal prognosis in these patients,<sup>39</sup> further research is needed to identify new noninvasive biomarkers. As automated segmentation tools are being developed,<sup>40</sup> these promising tools might also get integrated into standard practice in the future to detect early structural renal changes that would inform preventive or therapeutic strategies in CKD patients or patients treated with nephrotoxic agents. From a clinical perspective, this texture index might, thus, be used to help inform preventive strategies before reaching irreversible and severe nephrotoxicity. As such, it could represent an additional tool to help clinicians when facing the risk/benefit ratio issue of lithium discontinuation.

In conclusion, we developed and validated a non-invasive renal texture-based imaging index that may be relevant in the diagnosis and prognosis of lithium-induced renal toxicity, and ageing and chronic kidney disease. It might also provide insights on pathophysiological mechanisms leading to lithium nephrotoxicity in future studies.

## ACKNOWLEDGEMENTS

The authors wish to acknowledge the patients who accepted to enter the study, the nursing and medical staff who took care of the patients, and the technical staff who performed the imaging and the radioisotope measurements.

## CONFLICT OF INTEREST

The authors declare no conflict of interest.

## AUTHOR CONTRIBUTIONS

PB, MB, AD and NT designed the study. PB wrote the first draft of the manuscript. PB, LM, PF, EM, FB, BE, EVP, FV, MF and NT collected data. JPH performed the vasopressin plasma tests. MB, LC and NT analysed the data. PB conceived Figures 1 and 2. MB conceived Figure 3. NT conceived Figure 4. All the authors contributed to the analyses of the data and edited the manuscript.

## ORCID

Nahid Tabibzadeh  <https://orcid.org/0000-0001-5803-0163>

## REFERENCES

- Geddes JR, Burgess S, Hawton K, Jamison K, Goodwin GM. Long-term lithium therapy for bipolar disorder: systematic review and meta-analysis of randomized controlled trials. *Am J Psychiatry*. 2004;161(2):217-222.
- Cipriani A, Hawton K, Stockton S, Geddes JR. Lithium in the prevention of suicide in mood disorders: updated systematic review and meta-analysis. *BMJ*. 2013;27(346):f3646.
- Miura T, Noma H, Furukawa TA, et al. Comparative efficacy and tolerability of pharmacological treatments in the maintenance treatment of bipolar disorder: a systematic review and network meta-analysis. *Lancet Psychiatry*. 2014;1(5):351-359.
- Tabibzadeh N, Vrtovsnik F, Serrano F, Vidal-Petiot E, Flamant M. Chronic metabolic and renal disorders related to lithium salts treatment. *Rev Med Interne*. 2019;40(9):599-608.
- Shine B, McKnight RF, Leaver L, Geddes JR. Long-term effects of lithium on renal, thyroid, and parathyroid function: a retrospective analysis of laboratory data. *Lancet Lond Engl*. 2015;386(9992):461-468.
- McKnight RF, Adida M, Budge K, Stockton S, Goodwin GM, Geddes JR. Lithium toxicity profile: a systematic review and meta-analysis. *The Lancet*. 2012;379(9817):721-728.
- Davis J, Desmond M, Berk M. Lithium and nephrotoxicity: a literature review of approaches to clinical management and risk stratification. *BMC Nephrol*. 2018;19(1):305.
- Tabibzadeh N, Faucon A-L, Vidal-Petiot E, Serrano F, Males L, Fernandez P, et al. Kidney function and long-term treatment with lithium salts for bipolar disorder Determinants of mGFR and accuracy of kidney microcysts detection in the diagnosis of CKD [Internet]. 2021 Apr [cited 2021 Sep 8] p. 2021.04.11.21255136. <https://www.medrxiv.org/content/10.1101/2021.04.11.21255136v1>
- Markowitz GS, Radhakrishnan J, Kambham N, Valeri AM, Hines WH, D'agati VD. Lithium nephrotoxicity a progressive combined glomerular and tubulointerstitial nephropathy. *J Am Soc Nephrol*. 2000;11(8):1439-1448.
- Farres MT, Ronco P, Saadoun D, et al. Chronic lithium nephropathy: MR imaging for diagnosis. *Radiology*. 2003;229(2):570-574.
- Golshayan D, Nseir G, Venetz J-P, Pascual M, Barbey F. MR imaging as a specific diagnostic tool for bilateral microcysts in chronic lithium nephropathy. *Kidney Int*. 2012;81(6):601.
- Christensen BM, Marples D, Kim Y-H, Wang W, Frøkiaer J, Nielsen S. Changes in cellular composition of kidney collecting duct cells in rats with lithium-induced NDI. *Am J Physiol Cell Physiol*. 2004;286(4):C952-964.
- Christensen BM, Kim Y-H, Kwon T-H, Nielsen S. Lithium treatment induces a marked proliferation of primarily principal cells in rat kidney inner medullary collecting duct. *Am J Physiol-Ren Physiol*. 2006;291(1):F39-48.
- Lambin P, Leijenaar RTH, Deist TM, et al. Radiomics: the bridge between medical imaging and personalized medicine. *Nat Rev Clin Oncol*. 2017;14(12):749-762.
- Nath KA. Tubulointerstitial changes as a major determinant in the progression of renal damage. *Am J Kidney Dis*. 1992;20(1):1-17.

16. Menn-Josephy H, Lee CS, Nolin A, et al. Renal interstitial fibrosis: an imperfect predictor of kidney disease progression in some patient cohorts. *Am J Nephrol*. 2016;44(4):289-299.
17. Vidal-Petiot E, Courbebaisse M, Livrozet M, Corrége G, Rusu T, Montravers F, Baron S, Dupont L, Balouzet C, Smadja C, Leygnac S, Pariscoat G, Rose J, Rouzet F, Houillier P, Haymann J-P, Flamant M. Comparison of 51Cr-EDTA and 99mTc-DTPA for glomerular filtration rate measurement. *Journal of Nephrology*. 2021;34(3):729-737. <http://dx.doi.org/10.1007/s40620-020-00932-9>
18. Ho TA, Godefroid N, Gruzon D, et al. Autosomal dominant polycystic kidney disease is associated with central and nephrogenic defects in osmoregulation. *Kidney Int*. 2012;82(10):1121-1129.
19. Nuovo S, Fuiano L, Micalizzi A, et al. Impaired urinary concentration ability is a sensitive predictor of renal disease progression in Joubert syndrome. *Nephrol Dial Transplant*. 2020;35(7):1195-1202.
20. Fedorov A, Beichel R, Kalpathy-Cramer J, et al. 3D Slicer as an image computing platform for the Quantitative Imaging Network. *Magn Reson Imaging*. 2012;30(9):1323-1341.
21. van Griethuysen JJM, Fedorov A, Parmar C, et al. Computational radiomics system to decode the radiographic phenotype. *Cancer Res*. 2017;77(21):e104-e107.
22. Tibshirani R. Regression shrinkage and selection via the lasso. *J R Stat Soc Ser B Methodol*. 1996;58(1):267-288.
23. Grünfeld J-P, Rossier BC. Lithium nephrotoxicity revisited. *Nat Rev Nephrol*. 2009;5(5):270-276.
24. de Groot T, Ebert LK, Christensen BM, et al. Identification of Acer2 as a First Susceptibility Gene for Lithium-Induced Nephrogenic Diabetes Insipidus in Mice. *J Am Soc Nephrol JASN*. 2019;30(12):2322-2336.
25. Bankir L, Bouby N, Ritz E. Vasopressin: a novel target for the prevention and retardation of kidney disease? *Nat Rev Nephrol*. 2013;9(4):223-239.
26. Devuyst O, Wang X, Serra A. Vasopressin-2 receptor antagonists in autosomal dominant polycystic kidney disease: from man to mouse and back. *Nephrol Dial Transplant*. 2011;26(8):2423-2425.
27. Yoder BK. Role of primary cilia in the pathogenesis of polycystic kidney disease. *J Am Soc Nephrol JASN*. 2007;18(5):1381-1388.
28. Kline TL, Korfiatis P, Edwards ME, et al. Image texture features predict renal function decline in patients with autosomal dominant polycystic kidney disease. *Kidney Int*. 2017;92(5):1206-1216.
29. Zhang L, Chen Z, Feng L, et al. Preliminary study on the application of renal ultrasonography radiomics in the classification of glomerulopathy. *BMC Med Imaging*. 2021;21(1):115.
30. Amiri S, Akbarabadi M, Abdolali F, Nikoofar A, Esfahani AJ, Cheraghi S. Radiomics analysis on CT images for prediction of radiation-induced kidney damage by machine learning models. *Comput Biol Med*. 2021;133:104409.
31. Zhang G, Liu Y, Sun H, et al. Texture analysis based on quantitative magnetic resonance imaging to assess kidney function: a preliminary study. *Quant Imaging Med Surg*. 2021;11(4):1256-1270.
32. Bandara MS, Gurunayaka B, Lakraj G, Pallewate A, Siribaddana S, Wansapura J. Ultrasound Based Radiomics Features of Chronic Kidney Disease. *Academic Radiology*. 2022;29(2):229-235. <http://dx.doi.org/10.1016/j.acra.2021.01.006>
33. Srivastava A, Palsson R, Kaze AD, et al. The prognostic value of histopathologic lesions in native kidney biopsy specimens: results from the Boston kidney biopsy cohort study. *J Am Soc Nephrol JASN*. 2018;29(8):2213-2224.
34. Nicholson ML, McCulloch TA, Harper SJ, et al. Early measurement of interstitial fibrosis predicts long-term renal function and graft survival in renal transplantation. *Br J Surg*. 1996;83(8):1082-1085.
35. Farris AB, Adams CD, Broussides N, et al. Morphometric and visual evaluation of fibrosis in renal biopsies. *J Am Soc Nephrol JASN*. 2011;22(1):176-186.
36. Tabibzadeh N, Wagner S, Metzger M, et al. Fasting urinary osmolality, CKD progression, and mortality: a prospective observational study. *Am J Kidney Dis off J Natl Kidney Found*. 2019;73(5):596-604.
37. Berchtold L, Crowe LA, Friedli I, et al. Diffusion magnetic resonance imaging detects an increase in interstitial fibrosis earlier than the decline of renal function. *Nephrol Dial Transplant*. 2020;35(7):1274-1276.
38. Friedli I, Crowe LA, Berchtold L, et al. New magnetic resonance imaging index for renal fibrosis assessment: a comparison between diffusion-weighted imaging and T1 mapping with histological validation. *Sci Rep*. 2016;6(1):30088.
39. Farris AB, Colvin RB. Renal interstitial fibrosis: mechanisms and evaluation in: current opinion in nephrology and hypertension. *Curr Opin Nephrol Hypertens*. 2012;21(3):289-300.
40. Kim Y, Ge Y, Tao C, et al. Automated segmentation of kidneys from MR images in patients with autosomal dominant polycystic kidney disease. *Clin J Am Soc Nephrol CJASN*. 2016;11(4):576-584.

## SUPPORTING INFORMATION

Additional supporting information may be found in the online version of the article at the publisher's website.

**How to cite this article:** Beunon P, Barat M, Dohan A, et al. MRI-based kidney radiomic analysis during chronic lithium treatment. *Eur J Clin Invest*. 2022;52:e13756. doi:[10.1111/eci.13756](https://doi.org/10.1111/eci.13756)